2024 IEEE International Conference on Robotics and Automation (ICRA 2024)
May 13-17, 2024. Yokohama, Japan

A Large-area Tactile Sensor for Distributed Force Sensing Using Highly Sensitive Piezoresistive Sponge

Wendong Zheng, Kun Liu, Di Guo, Wuqiang Yang, Jun Zhu, and Huaping Liu*

***Abstract*— Tactile sensing plays a critical role in enabling robots to interact safely with target objects in dynamic and unstructured environments. While various tactile sensors based on different sensing principles or different sensitive materials have been proposed, the development of flexible large-area tactile sensors for robots is still challenging. In this paper, a novel highly sensitive piezoresistive sponge based on multi-walled carbon nanotubes (MWCNTs) and polyurethane (PU) sponge is fabricated for pressure sensing. The sensing behavior of the piezoresistive sponge was experimentally evaluated, showing high sensitivity and fast response. Based on the piezoresistive sponge, a flexible large-area tactile sensor is designed for distributed force detection with electrical resistance tomography technology. The sensing performance of the sensor is validated by touch location, sensitivity analysis, real-time touch discrimination, and touch modality recognition. The experimental results indicate that the sensor performs well in detecting the position and force of contact in a large area. The sensor's performance shows promise in embodied tactile sensing and human–robot interaction.**

I. Introduction

Tactile perception is crucial for robot physical interaction tasks [1] [2], primarily due to its ability to provide physical properties information of objects they interact with, which is not available through other sensing modalities [3] [4]. Therefore, tactile sensing has recently attracted much attention in the field of robotics [5] [6]. Various tactile sensors based on different sensing mechanisms and different sensing materials have been developed for robotic applications [7] [8] [9]. Although these tactile sensors have been successfully applied for some applications [10], most of them are limited to small-area robotic hands or fingers [11] [12].

As robots are increasingly deployed in dynamic scenarios, they require the ability to fully understand their surroundings and interact with them safely [13] [14]. To achieve this ability, large-area tactile sensors should be deployed on the robot body to detect a wide range of potential physical contacts throughout the sensing area [15] [16]. Therefore, there is increasing interest in developing large-area tactile sensors [17] [18]. While several large-area tactile sensors have been reported, most of them are implemented using array-based sensing methods. Specifically, these sensors consist of a series of discrete sensing units, each unit responsible for an area. However, the application of this type of sensor is limited when the amount of sensing elements required is large [19]. Therefore, the deployment of large-scale tactile sensors on the robot surface based on array-based structures is not realistic [20] [21].

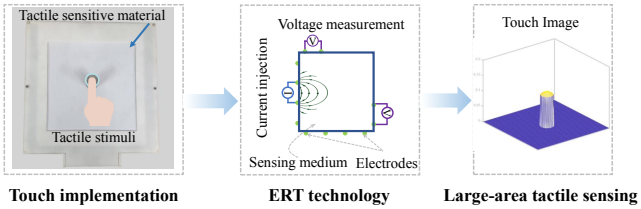

Fig. 1. An illustration of large-area tactile sensing based on ERT.

Electrical Resistance Tomography (ERT) is a non-invasive imaging technique that estimates the internal conductivity distribution of a sensing medium [22]. This is achieved by collecting measurements from boundary electrodes and using the measurement data to reconstruct a conductivity distribution [23]. ERT offers several benefits, including large-area scalability and durability, making it suitable for practical deployment in sensing applications [24]. By deploying ERT on a stretchable conductive medium, it becomes feasible to develop flexible sensors with arbitrary size and shape. This characteristic of ERT holds great promise for implementing large-scale tactile sensing [25].

Recently, ERT technology for tactile sensing has emerged as a promising solution to overcome the limitations associated with traditional array-based sensing methods [26] [27]. Over the past few years, there has been significant progress in the development of ERT-based tactile sensors. Researchers have been exploring and utilizing various conductive materials to create tactile sensors that can be applied in various contexts and for diverse applications [28] [29] [30]. Most ERT-based tactile sensors have utilized the conductivity changes of conductive fabrics to measure the applied pressure distribution, yielding promising results in specific applications. However, it is important to note that

Wendong Zheng is with the School of Electrical Engineering and Automation, Tianjin University of Technology, Tianjin, China, and also with the Department of Computer Science and Technology, Tsinghua University, Beijing, China.

Kun Liu is with the State Key Laboratory on Integrated Optoelectronics, Institute of Semiconductors, Chinese Academy of Sciences, University of Chinese Academy of Sciences, Beijing, China.

Di Guo is with the School of Artificial Intelligence, Beijing University of Posts and Telecommunications, Beijing, China.

Wuqiang Yang is with the Department of Electrical and Electronic Engineering, The University of Manchester, Manchester M13 9PL, U.K.

Jun Zhu is with the School of Automation, Nanjing University of Information Science and Technology, Nanjing, China.

Huaping Liu is with the Department of Computer Science and Technology, Tsinghua University, Beijing, China, and also with Beijing National Research Center for Information Science and Technology, China.

This work was completed while Wendong Zheng was a postdoctor in the Department of Computer Science and Technology, Tsinghua University, and Jun Zhu was visiting Tsinghua University.

*Corresponding author: Huaping Liu (hpliu@tsinghua.edu.cn).

the sensitivity of these sensors to pressure can be limited by the inherent properties of the fabric, including its electrical conductivity and modulus of compressive elasticity.

On the other hand, the porous polyurethane (PU) sponge has great application potential in flexible sensors [31]. Several existing studies have demonstrated that sponge sensors with unique three-dimensional structures can exhibit high sensitivity to pressure. Furthermore, the flexible and lightweight nature of sponge sensors is an additional advantage. However, it should be noted that most existing research on sponge sensors has primarily focused on their piezoresistive properties as individual units, rather than on large-area tactile sensing. This significantly limits the potential applications of sponge sensors. Consequently, developing a high-performance large-area tactile sensor remains a challenging task.

In this study, our objective is to develop a flexible large-area tactile sensor specifically designed for robot sensing applications. To this end, a novel highly sensitive piezoresistive sponge based on MWCNTs and PU sponge is first fabricated for pressure sensing. The sensing behavior of the piezoresistive sponge is evaluated by experiments. Based on the piezoresistive sponge, we develop a novel flexible large-area tactile sensor for distributed force detection, with electrical resistance tomography technology, as shown in Fig.1. In order to verify the effectiveness of the proposed sensor, a series of experiments are conducted. The main contributions are summarized as follows.

1) A novel piezoresistive sponge has been developed using MWCNTs and PU sponge for pressure sensing. Compared to pressure sensors formed of conductive fabric and conductive rubber, piezoresistive sponges offer significant advantages including high sensitivity and good flexibility. Moreover, it has low-cost fabrication and a simple structure, which can easily be tailored to meet particular application requirements.
2) We develop a novel large-area tactile sensor for distributed force detection by integrating the previously mentioned sponge with ERT technology. Compared with existing array-based tactile sensors, our method offers the advantage of achieving large-area tactile perception without the limitations of complicated internal wiring. This makes it particularly attractive for robot tactile skins that cover the entire robot body.
3) The prototype of the large-area tactile sensor has been fabricated, and its sensing performance has been evaluated. The experimental results demonstrate that the sensor exhibits excellent sensing capabilities.

II. High-Performance Piezoresistive Sponge

A. Fabrication Procedure

A 2 mm thick polyurethane (PU) sponge is employed as the flexible porous scaffold. This selection was made due to the advantageous properties including large specific surface area and excellent elasticity. MWCNTs is utilized as conductive filler due to its high aspect ratio. By incorporating MWCNTs into the PU sponge, the resulting composite material exhibits piezoresistive properties.

The fabrication procedure of the piezoresistive sponge is illustrated in Fig.2. Firstly, the sponge is cut into a pre-specified shape using a laser cutter. Secondly, it is cleaned with propanol, followed by ethanol, and then deionized water under ultrasonication. Then, the cleaned sponge is dried in an oven at 70 °C for one hour. Afterward, the sponge that has been treated is put into an aqueous dispersion of MWCNTs for five minutes, allowing the MWCNTs to be dip-coated onto the inside of the sponge. Finally, the sponge is subjected to sonication to remove the remaining liquid and then dried on a heating platform. The two processes are repeated several times to ensure that the MWCNTs particles are well deposited on the sponge skeleton.

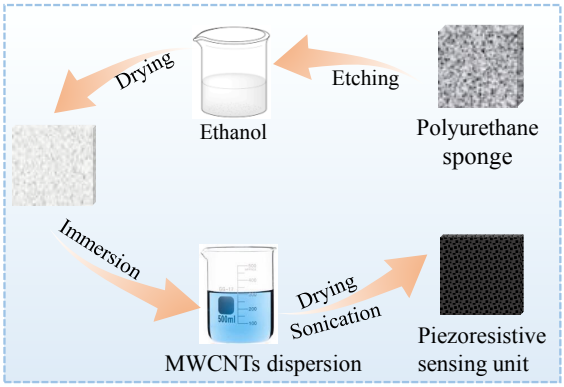

Fig. 2. Fabrication procedure of the piezoresistive sponge

B. Sensing Properties of the Piezoresistive Sponge

The MWCNTs-coated PU sponge is used as the conductive layer of the tactile sensor, which plays an essential role in the sensor. To study the sensing properties of the sponge, a 1.5cm×1.5cm flexible pressure sensor is created by attaching the piezoresistive sponge to two copper electrodes and covering it with a polyethylene terephthalate film.

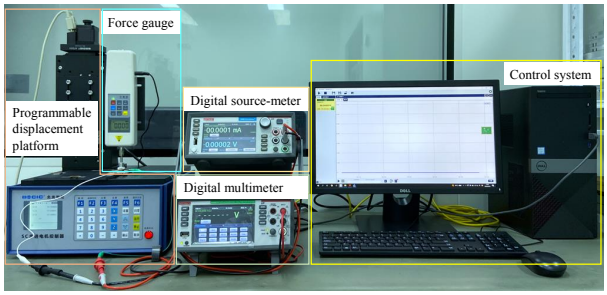

Fig. 3. Experiment platform for testing the sensing properties of piezoresistive sponges.

An experimental platform is built to test the sensing properties of the piezoresistive sponge, as shown in Fig.3. It consists of a force gauge (HEMUELE, SH-50), a digital source meter (KEITHLEY, 2450), a digital multimeter (KEITHLEY, DAQ6510), a programmable movable platform (MVS405),

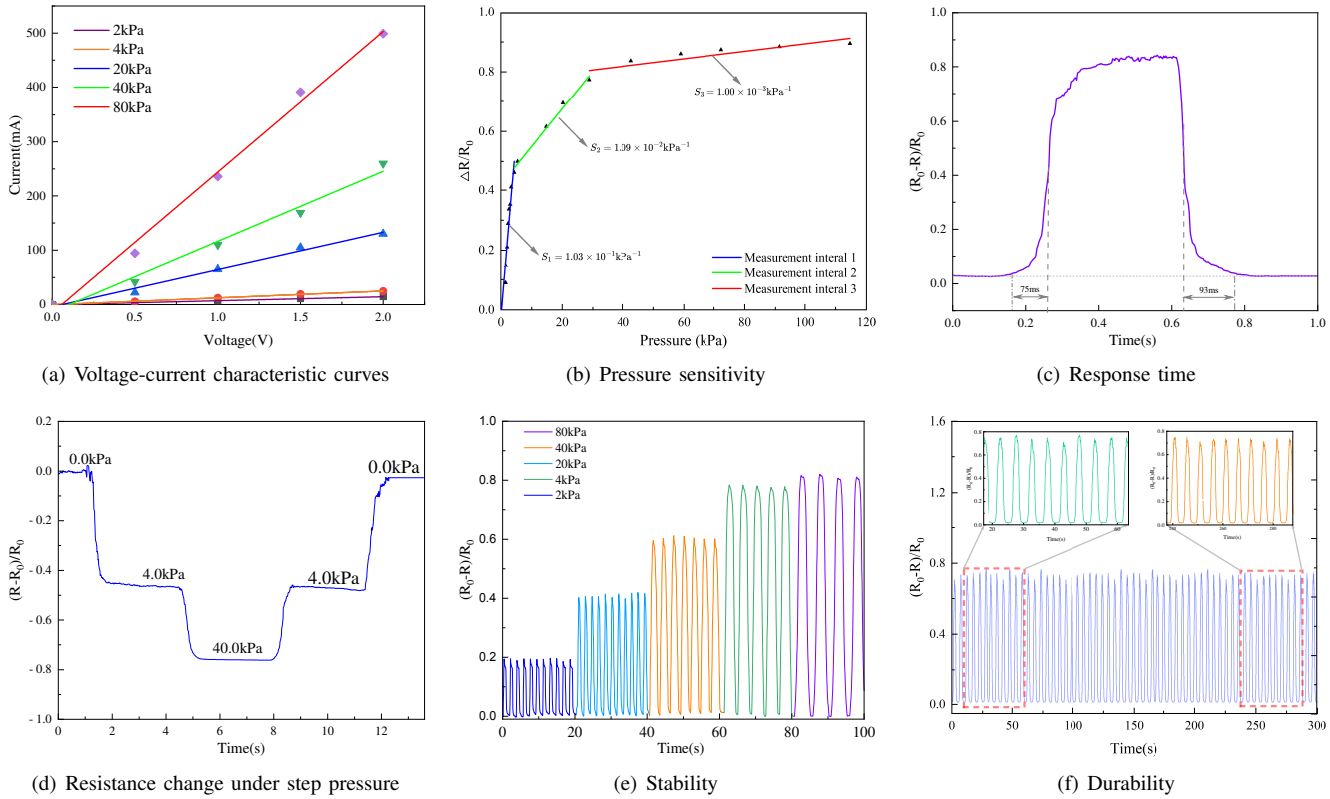

(a) Voltage-current characteristic curves (b) Pressure sensitivity (c) Response time

(d) Resistance change under step pressure (e) Stability (f) Durability

Fig. 4. Sensing properties of the piezoresistive sponge.

and a computer control system. The force gauge is installed on the movable platform controlled by the computer. The flexible pressure sensor is fixed on the base of the movable platform.

The relationship between the current response and the input voltage under different applied pressures is shown in Fig. 4(a). It can be seen that all the results exhibit a good linear relationship in the voltage range of $0 - 2$V under different pressures from 2 to 80kPa, showing a stable response. Additionally, with increasing applied pressure, the slope of the current-voltage curve increases accordingly, indicating that the resistance of the sensor decreases with an increase in applied pressure. The experimental results are consistent with the theoretical analysis.

Pressure sensitivity is a fundamental parameter for evaluating the performance of a pressure sensor. Fig. 4(b) illustrates the relationship between the rate of resistance change $\Delta R/R_0 = (R_0 - R)/R_0$ and the applied pressure, where R_0 and R denote resistance without and with pressure, respectively. From Fig.4(b), it can be observed that the curve exhibits three linear regions with different sensitivity within the pressure range of 0-116 kPa: 0.103 kPa^{-1} in the low-pressure region (0-4 kPa), 0.0109 kPa^{-1} in the medium-pressure region (4-30 kPa), and 0.001 kPa^{-1} in the high-pressure region (30-116 kPa). Comparing our pressure sensitivity (0.103 kPa^{-1}) to other nanocomposite sensors (ranging from 0.103 kPa^{-1} to 0.33 kPa^{-1}), our sensor exhibits favorable sensitivity. Additionally, our pressure sensitivity is higher than previously reported ones, which ranged from 0.001 kPa^{-1} to 0.088 kPa^{-1} [32]. This result confirms that our sensor demonstrates high sensitivity to compressive pressure within a specific range.

Response and recovery time are also important parameters to evaluate sensor performance. The response time indicates how quickly a sensor can detect and respond to an applied pressure, while the recovery time measures how rapidly the sensor returns to its original state after the pressure is removed. Fig.4(c) illustrates the response and recovery times of the sensor when subjected to a pressure of 20 kPa. As shown in Fig.4(c), the response time is approximately 75 ms, while the recovery time is around 93 ms. These values indicate that the sensor exhibits a good response performance, making it suitable for real-time tactile measurements required in robotic applications.

Fig.4(d) shows the change in resistance of the sensor under step pressure. In this experiment, pressure is gradually applied to the sensor from 4 kPa to 40 kPa, and then the pressure is gradually released. From Fig.4(d), It can be seen that the resistance change rates remain consistent under the same pressure during the loading and unloading processes. This indicates that the sensor maintains high stability even after undergoing step pressure processes.

The stability experiment is conducted using the sensor, applying pressures of 2, 4, 20, 40, and 80 kPa, respectively. The stability experiment data is presented in Fig.4(e). The results reveal excellent stability under all five different pres-

sures, with the resistance change rate gradually increasing as the pressure increases.

Long-term durability is an important aspect for practical applications of sensors. Fig.4(f) shows the results of thousands of dynamic loading and unloading tests carried out under a specific pressure. These results demonstrate that the sensor maintains excellent stability and durability throughout the tests.

These experimental results confirm the sensor's excellent sensitivity and stability across a wide range of pressures. Additionally, the piezoresistive sponge is low-cost and can be easily scaled up. This makes it a promising option for realizing large-area tactile sensing.

III. Fabrication of Flexible Large-area Tactile Sensor

Based on the research in Section II, a large area tactile sensor is designed and fabricated by utilizing the piezoresistive sponge and employing electrical resistance tomography, as illustrated in Fig.1.

A. Theoretical Backgrounds of ERT

To comprehend the principles of ERT for tactile sensing, it is essential to understand the forward and inverse problems involved, which elucidate the connection between the measured voltage and the conductivity distribution.

The ERT method relies on Maxwell's equations, which establish the connection between conductivity σ and voltage potential u within a closed bounded domain Ω.

$$\sigma \nabla^2 u = 0 \quad \text{in} \quad \Omega \tag{1}$$

When a current is injected into the boundary domain $\partial\Omega$, the boundary condition can be expressed as follows:

$$\sigma \nabla u \cdot \mathbf{n} = j_l \quad \text{on} \quad \partial\Omega \tag{2}$$

where j_l is the current density at electrode e_l, and n is unit vector normal to $\partial\Omega$.

By combining equation (1) and (2), the voltage at the boundary V_l can be calculated based on a given conductivity distribution σ and the injection current density j_l. This represents the forward problem of ERT. In practical applications, the finite element method (FEM) is usually used to solve this problem.

In ERT, the primary concern is how to determine the conductivity distribution σ based on the boundary voltage measurements V. In the context of tactile sensing, the ultimate objective is to determine the change in conductivity $\delta\sigma$ based on the change in boundary voltage δV. However, this is an ill-posed and nonlinear inverse problem. To tackle this problem, a linear approximation can be employed to describe the relationship between $\delta\sigma$ and δV:

$$\delta V = J\delta\sigma + \varepsilon \tag{3}$$

where J is the Jacobian matrix, which can be calculated from the finite element model, and ε is measurement noise. By computing the pseudo-inverse with a regularization term, the solution of $\delta\sigma$ can be expressed as:

$$\delta\sigma = (J^T J + \lambda^2 R^T R)^{-1} J^T \delta V \tag{4}$$

where R is the regularization matrix, and λ is the regularization hyperparameter. For more detailed information, you can refer to [33].

B. Fabrication Process

Taking advantage of the benefits offered by a multilayered structure for sensing distributed force over a large area, the tactile sensor is designed using multiple layers as depicted in Fig.5. The sensor comprises a base layer, which is a $20 \times 20cm^2$ flexible printed circuit. On the boundary of the base layer, 16 electrodes are evenly arranged. Following our previous work [24], a sensing domain is fabricated on the base layer by spray coating it with carbon black (CRAMOLIN 1281411). The sprayed layer is carefully controlled to achieve a conductivity of approximately 0.006 S/m.

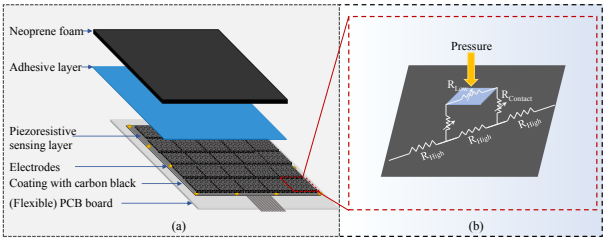

Fig. 5. Schematic diagram of the structure of the tactile sensor

To effectively detect multiple simultaneous touches, the piezoresistive sensing layer is constructed using discrete sponge sensing units instead of a monolithic piezoresistive sponge. This design is primarily motivated by the ability of the lattice structure to prevent current flow between different touch points through the sensing layer. The sensing units are designed to have dimensions of $7.5 \times 7.5mm^2$ and fabricated using the production process described in section II-A. Subsequently, an array of these sensing units, measuring 24×24, is attached to the neoprene foam using an adhesive to create the upper layer of the sensor. Finally, the upper layer is placed on top of the base layer and secured with adhesive tape, resulting in the complete assembly of the sensor. The fabrication process described above ensures that the sensor is inherently soft and flexible. This characteristic makes it highly suitable for deployment on robot surfaces.

C. Data Acquisition System

A data acquisition system is developed for the sensor using a combination of a commercial data acquisition card (NET6024-S) and a customized multiplexing board. The electrodes of the sensor are connected to two multiplexers (MAX306) integrated into the multiplexer board. At the same time, these multiplexers are connected to a current driver and the data acquisition unit. During sensor operation, the selection of electrodes is performed by the multiplexers, which are controlled by a microcontroller STM32F107.

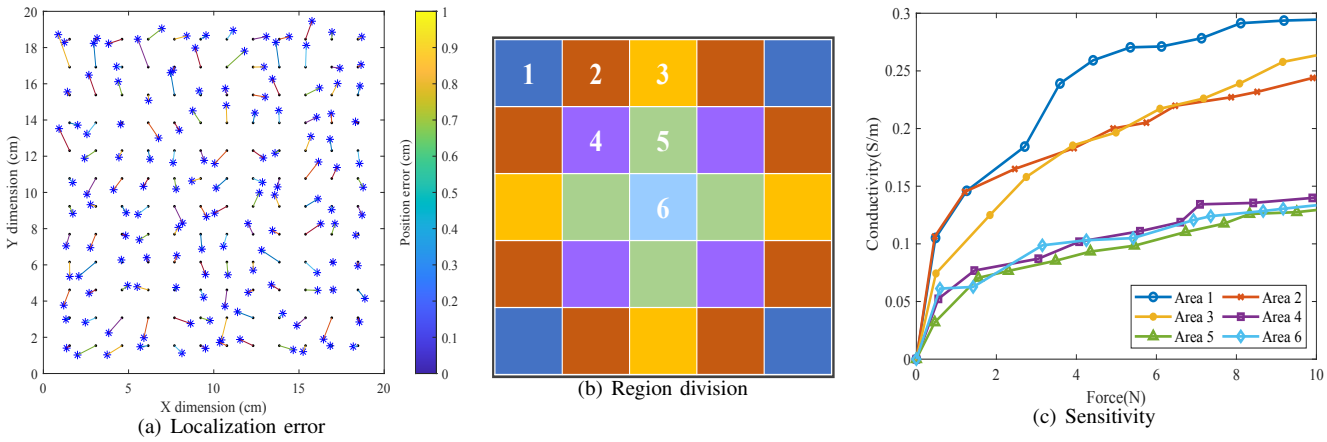

(a) Localization error (b) Region division (c) Sensitivity

Fig. 6. Performance evaluation of the tactile sensor.

A pairwise injection pattern is employed for the ERT sensor. To enable easy integration of the sensor into robotic applications, a battery and a voltage-current module are utilized to provide current excitation for the sensor. For voltage measurement, the parallel acquisition method is adopted, which not only effectively improves the acquisition efficiency, but also reduces the time difference between the data of all channels.

IV. Performance Evaluation

To evaluate the sensing performance of the sensor, experiments are conducted. Given the focus of our work on studying the novel sensor for large-area tactile sensing, the traditional reconstruction algorithm Newton's one-step error reconsruction (NOSER) is employed to reconstruct conductivity images from the acquired data.

A. Location Performance Analysis

For large-area tactile sensing, location performance is crucial in practical applications. To evaluate the sensor's location accuracy, experiments are conducted at 81 different locations on the sensor surface, applying pressure through point contact. To mitigate the influence of noise, the conductivity images are processed by applying a threshold of 25% of the maximum value. The contact position is then determined using a weighted centroid calculation.

The location error is quantified by calculating the Euclidean distance between the actual indentation point and the calculated centroid. The experimental results of location error are shown in Fig. 6(a). In the figure, black dots represent the centroids of the target positions, while blue asterisks represent the centroids of the contact locations measured by the sensor. The results indicate that although there is some location error, the sensor is capable of accurately measuring the contact location.

B. Sensitivity Analysis

To further assess the performance of the sensor, the sensitivity of the sensor is analyzed. Considering the location dependence of the ERT-based tactile sensor, the entire sensing area is divided into a virtual array of dimensions 5×5. Taking into account the sensor's symmetry, these 25 sensing areas are further categorized into six regions, as depicted in Fig.6(b). Regions with the same color represent areas with similar tactile sensitivity.

The relationship between the peak value of the reconstructed conductivity image and contact force is shown in Fig. 6(c). In this figure, the peak values of conductivity are averaged across the entire sensing area. From Fig. 6(c), it can be seen that within the range of 1-10N, the conductivity value increases with the increase of pressure. This demonstrates that the sensor is sensitive to variations in pressure and can effectively detect and quantify the magnitude of the contact force.

C. Pressure Distribution Imaging

To validate the sensor's ability to effectively detect touch contact and achieve multi-target detection, a series of single-target and multi-target detection experiments are performed. In these experiments, a 100g weight was used to apply contact force to the sensor. The experiment results are shown in Fig.7.

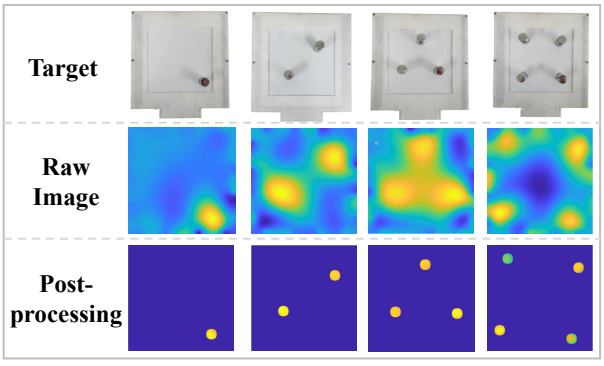

Fig. 7. Single-target and multiple-target touch image.

In the case of single-target pressure, the raw image clearly indicates the position of the applied pressure, demonstrating

the effectiveness of the tactile sensor in detecting pressure. In multi-target scenarios, although the initially reconstructed images may contain some artifacts or imperfections, effective recognition of contact points is still achievable through post-processing.

For ERT-based sensors, implementing multi-point detection is challenging as applying pressure at multiple points can often lead to error collapse. However, despite the challenge, the experimental results demonstrate that the developed sensor is still capable of effectively detecting multiple-target contacts. The effectiveness of the developed sensor is further verified.

D. Real-time Touch Discrimination

To evaluate the sensor's real-time performance in real applications, we conducted experiments to detect hand-touch contacts, which are commonly encountered in human-robot interaction scenarios. When a fingertip applies force to the sensor, a 3D image can be generated, as illustrated in Fig.8. By analyzing the touch image, some quantitative information about touch can be obtained, including touch positions, contact intensity, and contact area. From Fig. 8, it can be seen that the height of the image increases the applied contact force, indicating that our sensor can accurately measure the distribution of forces in real-time.

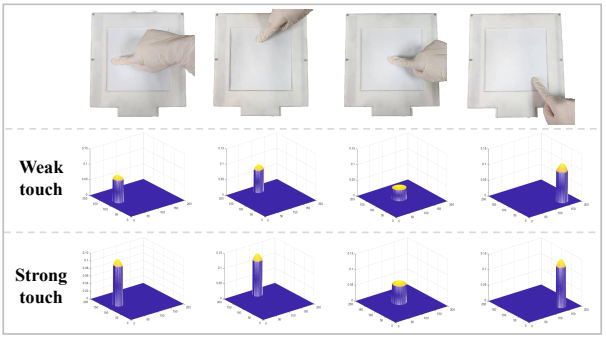

Fig. 8. Real-time touch discrimination.

E. Touch Modality Recognition

In order to demonstrate the sensor's applicability in the field of human-robot interaction, a touch modality discrimination experiment is conducted. This experiment aimed to classify eight different types of touch that commonly occur in real-world human-robot interaction scenarios. It is shown in Fig. 9.

To evaluate the recognition accuracy, we conducted an experiment using actual measurement data, where a Deep Neural Network (DNN) model was applied. In Fig.10, we present the confusion matrix results obtained from the touch modality discrimination experiment. The results demonstrate a high recognition accuracy of 97.9% for the testing dataset. This indicates that the sensor, when coupled with the DNN model, can effectively identify and discriminate between various touch modalities. This confirms the feasibility of the sensor in touch interaction.

(a) 1-point touch (b) 2-point touch (c) 3-point touch (d) 4-point touch

(e) Finger-pressing (f) Hand pressing (g) L-shaped touch (h) Palm pressing

Fig. 9. Eight different types of touch.

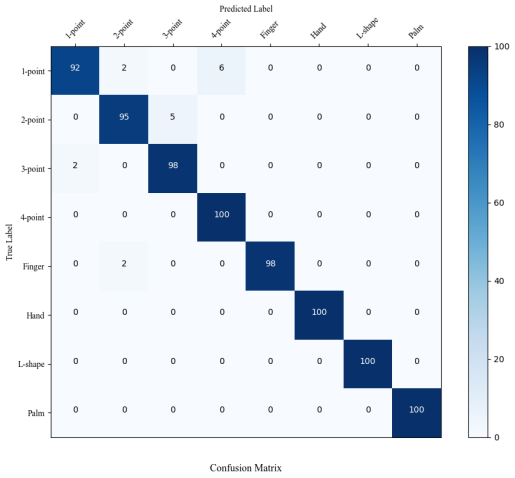

Fig. 10. Confusion matrix results of touch modality recognition.

V. Conclusions

A fabrication method is proposed for a highly sensitive piezoresistive sponge based on MWCNTs and PU sponge. By combining the custom-made piezoresistive sponge and ERT, a novel large-area flexible tactile sensor is developed for robotic perception. Experimental results demonstrate the effectiveness of the proposed sensor in large-area tactile sensing. Due to its low cost and easy fabrication, the sensor has promising potential for practical applications in the field of tactile sensing.

Since this work primarily focuses on investigating a novel large-area tactile sensor, the traditional algorithm is employed to solve the inverse problem. In the future, we will explore and develop imaging reconstruction methods specifically tailored for tactile sensing to further enhance the performance of the sensor.

Acknowledgment

This work was supported by the National Natural Science Fund for Key International Collaboration under Grant 62120106005 and the National Natural Science Foundation of China under Grant 62303259.

REFERENCES

[1] F. Liu, S. Deswal, A. Christou, Y. Sandamirskaya, M. Kaboli, and R. Dahiya, "Neuro-inspired electronic skin for robots," *Science Robotics*, vol. 7, no. 67, p. eabl7344, 2022.

[2] M. Johnsson and C. Balkenius, "Sense of touch in robots with self-organizing maps," *IEEE Transactions on Robotics*, vol. 27, no. 3, pp. 498–507, 2011.

[3] Q. Li, O. Kroemer, Z. Su, F. F. Veiga, M. Kaboli, and H. J. Ritter, "A review of tactile information: Perception and action through touch," *IEEE Transactions on Robotics*, vol. 36, no. 6, pp. 1619–1634, 2020.

[4] W. Zheng, H. Liu, B. Wang, and F. Sun, "Cross-modal surface material retrieval using discriminant adversarial learning," *IEEE transactions on industrial informatics*, vol. 15, no. 9, pp. 4978–4987, 2019.

[5] H. Liu, D. Guo, and F. Sun, "Object recognition using tactile measurements: Kernel sparse coding methods," *IEEE Transactions on Instrumentation and Measurement*, vol. 65, no. 3, pp. 656–665, 2016.

[6] S. Luo, J. Bimbo, R. Dahiya, and H. Liu, "Robotic tactile perception of object properties: A review," *Mechatronics*, vol. 48, pp. 54–67, 2017.

[7] Z. Lin, J. Zhuang, Y. Li, X. Wu, S. Luo, D. F. Gomes, F. Huang, and Z. Yang, "Gelfinger: A novel visual-tactile sensor with multi-angle tactile image stitching," *IEEE Robotics and Automation Letters*, 2023.

[8] W. Zheng, B. Wang, H. Liu, X. Wang, Y. Li, and C. Zhang, "Bio-inspired magnetostrictive tactile sensor for surface material recognition," *IEEE Transactions on Magnetics*, vol. 55, no. 7, pp. 1–7, 2019.

[9] H. Qiao, "Robotic intelligence and automation," *Robotic Intelligence and Automation*, vol. 43, no. 1, pp. 1–2, 2023.

[10] H. Sun, K. J. Kuchenbecker, and G. Martius, "A soft thumb-sized vision-based sensor with accurate all-round force perception," *Nature Machine Intelligence*, vol. 4, no. 2, pp. 135–145, 2022.

[11] H. Lee, K. Park, J. Kim, and K. J. Kuchenbecker, "Internal array electrodes improve the spatial resolution of soft tactile sensors based on electrical resistance tomography," in *2019 International Conference on Robotics and Automation (ICRA)*. IEEE, 2019, pp. 5411–5417.

[12] B. Fang, Z. Xia, F. Sun, Y. Yang, H. Liu, and C. Fang, "Soft magnetic fingertip with particle-jamming structure for tactile perception and grasping," *IEEE Transactions on Industrial Electronics*, vol. 70, no. 6, pp. 6027–6035, 2022.

[13] S. Yang, W. Zhang, R. Song, J. Cheng, H. Wang, and Y. Li, "Watch and act: Learning robotic manipulation from visual demonstration," *IEEE Transactions on Systems, Man, and Cybernetics: Systems*, 2023.

[14] H. Qiao, Y.-X. Wu, S.-L. Zhong, P.-J. Yin, and J.-H. Chen, "Brain-inspired intelligent robotics: Theoretical analysis and systematic application," *Machine Intelligence Research*, vol. 20, no. 1, pp. 1–18, 2023.

[15] A. Schmitz, P. Maiolino, M. Maggiali, L. Natale, G. Cannata, and G. Metta, "Methods and technologies for the implementation of large-scale robot tactile sensors," *IEEE Transactions on Robotics*, vol. 27, no. 3, pp. 389–400, 2011.

[16] H. Liu, D. Guo, F. Sun, W. Yang, S. Furber, and T. Sun, "Embodied tactile perception and learning," *Brain Science Advances*, vol. 6, no. 2, pp. 132–158, 2020.

[17] Z. Si, T. C. Yu, K. Morozov, J. McCann, and W. Yuan, "Robotsweater: Scalable, generalizable, and customizable machine-knitted tactile skins for robots," *arXiv preprint arXiv:2303.02858*, 2023.

[18] Y. Zhang, Z. Lin, X. Huang, X. You, J. Ye, and H. Wu, "A large-area, stretchable, textile-based tactile sensor," *Advanced Materials Technologies*, vol. 5, no. 4, p. 1901060, 2020.

[19] H. Chen, X. Yang, P. Wang, J. Geng, G. Ma, and X. Wang, "A large-area flexible tactile sensor for multi-touch and force detection using electrical impedance tomography," *IEEE Sensors Journal*, vol. 22, no. 7, pp. 7119–7129, 2022.

[20] K. Park, H. Lee, K. J. Kuchenbecker, and J. Kim, "Adaptive optimal measurement algorithm for ert-based large-area tactile sensors," *IEEE/ASME Transactions on Mechatronics*, vol. 27, no. 1, pp. 304–314, 2021.

[21] Y. Li, J. Zhang, J. Yi, and K. Zhang, "Convolutional-generative adversarial network: Data-driven mechanical inverse method for intelligent tactile perception," *Advanced Intelligent Systems*, p. 2100187, 2022.

[22] D. Silvera-Tawil, D. Rye, M. Soleimani, and M. Velonaki, "Electrical impedance tomography for artificial sensitive robotic skin: A review," *IEEE Sensors Journal*, vol. 15, no. 4, pp. 2001–2016, 2015.

[23] K. Park, H. Yuk, M. Yang, J. Cho, H. Lee, and J. Kim, "A biomimetic elastomeric robot skin using electrical impedance and acoustic tomography for tactile sensing," *Science Robotics*, vol. 7, no. 67, p. eabm7187, 2022.

[24] W. Zheng, H. Liu, D. Guo, and W. Yang, "Adaptive optimal electrical resistance tomography for large-area tactile sensing," in *2023 IEEE International Conference on Robotics and Automation (ICRA)*. IEEE, 2023, pp. 10 338–10 344.

[25] H. Mitsubayashi, S. Yoshimoto, and A. Yamamoto, "Adaptive potential scanning for a tomographic tactile sensor with high spatio-temporal resolution," in *2020 IEEE/RSJ International Conference on Intelligent Robots and Systems (IROS)*. IEEE, 2020, pp. 9827–9832.

[26] D. Silvera Tawil, D. Rye, and M. Velonaki, "Interpretation of the modality of touch on an artificial arm covered with an eit-based sensitive skin," *The International Journal of Robotics Research*, vol. 31, no. 13, pp. 1627–1641, 2012.

[27] A. Yao, C. L. Yang, J. K. Seo, M. Soleimani *et al.*, "Eit-based fabric pressure sensing," *Computational and mathematical methods in medicine*, vol. 2013, 2013.

[28] S. Yoshimoto, Y. Kuroda, and O. Oshiro, "Tomographic approach for universal tactile imaging with electromechanically coupled conductors," *IEEE Transactions on Industrial Electronics*, vol. 67, no. 1, pp. 627–636, 2018.

[29] X. Duan, S. Taurand, and M. Soleimani, "Artificial skin through super-sensing method and electrical impedance data from conductive fabric with aid of deep learning," *Scientific reports*, vol. 9, no. 1, pp. 1–11, 2019.

[30] H. Zhao and W. Yang, "Flexible tactile sensing based on electrical resistance tomography and wavelet image fusion," in *2021 IEEE International Conference on Imaging Systems and Techniques (IST)*. IEEE, 2021, pp. 1–6.

[31] Z. Ye, G. Pang, K. Xu, Z. Hou, H. Lv, Y. Shen, and G. Yang, "Soft robot skin with conformal adaptability for on-body tactile perception of collaborative robots," *IEEE Robotics and Automation Letters*, vol. 7, no. 2, pp. 5127–5134, 2022.

[32] M. Xu, F. Li, Z. Zhang, T. Shen, Q. Zhang, and J. Qi, "Stretchable and multifunctional strain sensors based on 3d graphene foams for active and adaptive tactile imaging," *Science China Materials*, vol. 62, no. 4, pp. 555–565, 2018.

[33] D. Silvera-Tawil, D. Rye, M. Soleimani, and M. Velonaki, "Electrical impedance tomography for artificial sensitive robotic skin: A review," *IEEE Sensors Journal*, vol. 15, no. 4, pp. 2001–2016, 2014.